

iScience, Volume 26

Supplemental information

Ventral pallidal glutamatergic neurons

regulate wakefulness and emotion

through separated projections

Yan-Jia Luo, Jing Ge, Ze-Ka Chen, Zi-Long Liu, Michael Lazarus, Wei-Min Qu, Zhi-Li Huang, and Ya-Dong Li

Supplementary figures and legends

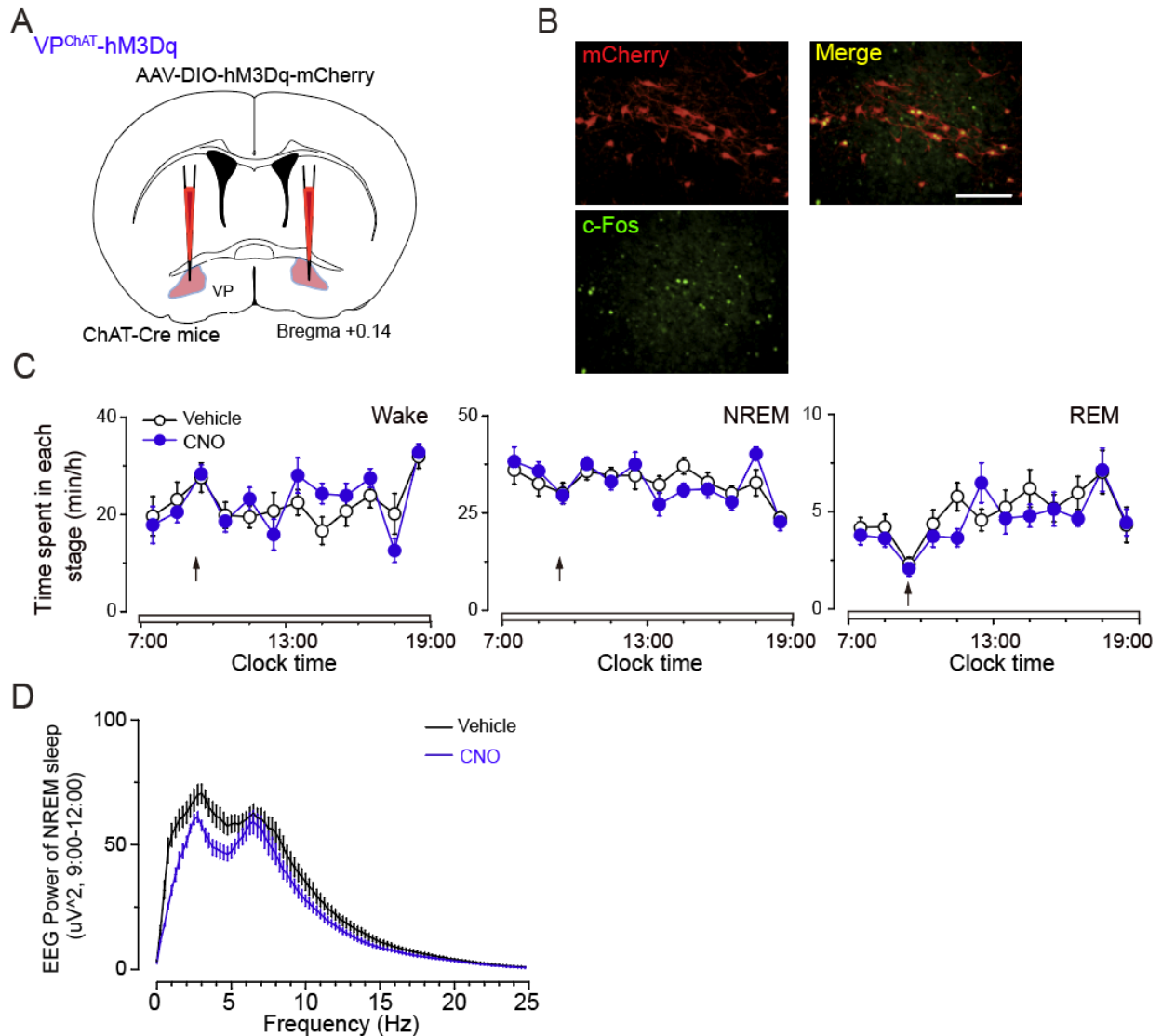


Figure S1. Chemogenetic activation of VP^{ChAT} neurons did not alter sleep-wake amount or EEG power density, Related to Figure 2.

(A) Schematic diagram of chemogenetic activation of VP cholinergic neurons in ChAT-Cre mice. (B) c-Fos expression in mCherry+ neurons 1.5 hours after CNO 1 mg/kg i.p. injection. Scale bar = 100 μ m. (C) Time-course of wakefulness, NREM sleep, and REM sleep after administration of vehicle or CNO. (D) EEG power spectrum from 9:00-12:00

after administration of vehicle or CNO (n = 6 mice; repeated-measures ANOVA followed by Tukey *post-hoc* test).

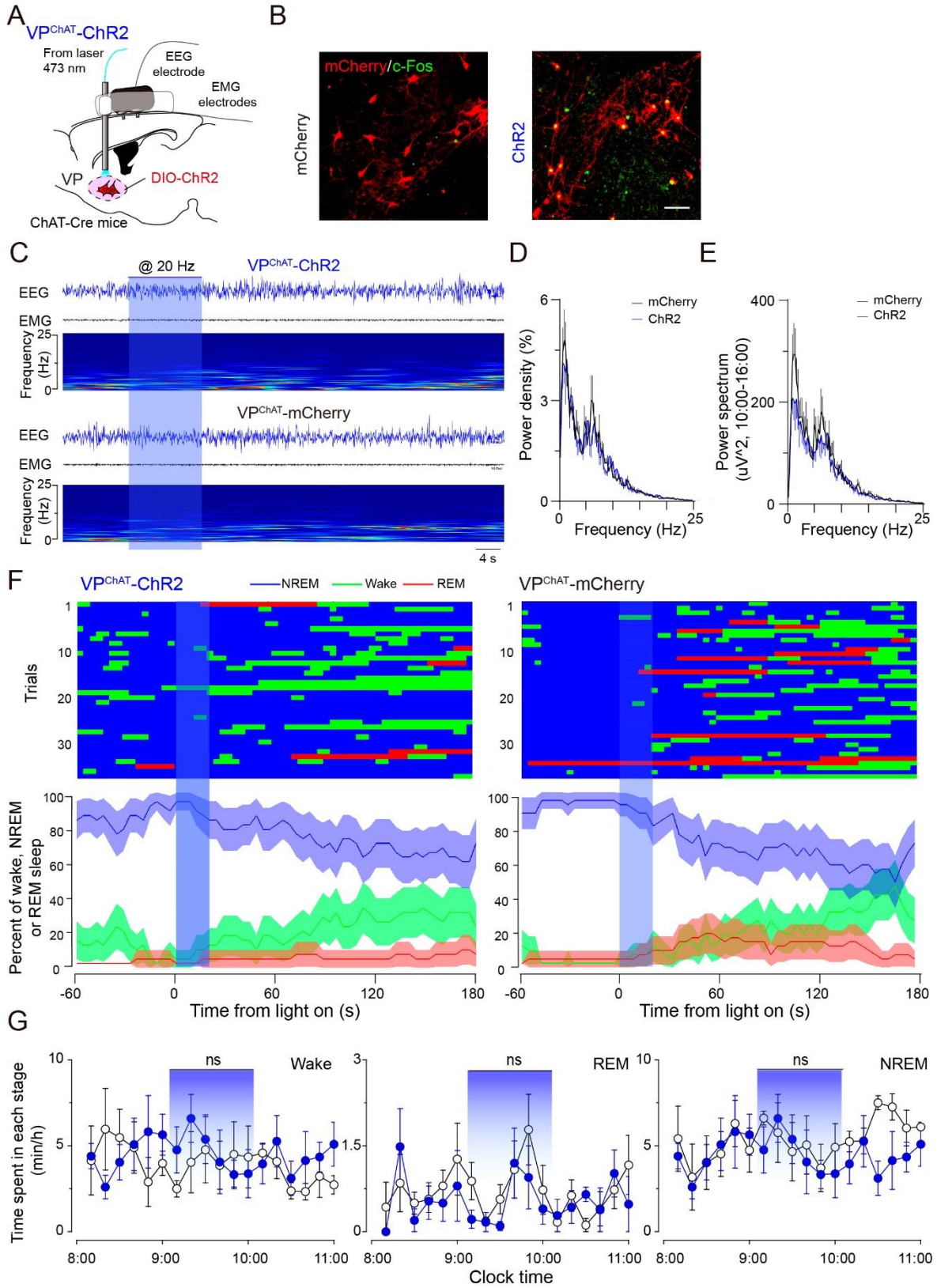


Figure S2. Optogenetic activation of VP^{ChAT} neurons does not change sleep-wake states, Related to Figure 2. (A) Sagittal diagram for *in vivo* optogenetic stimulation of VP^{ChAT} neurons in ChAT-Cre mice. (B) c-Fos expression in mCherry+ neurons after one-hour light stimulation. Scale bar = 50 μ m. (C) Optogenetic activation of VP^{ChAT} neurons did not change sleep stages. Heatmap of EEG and representative traces of EEG/EMG recordings in a ChAT-Cre mouse expressing ChR2-mCherry (upper) or mCherry (below). (D–E) EEG power density (D) and power spectrum (E) during optogenetic stimulation of VP^{ChAT} neurons. (F) Sleep stage after blue-light stimulation of VP^{ChAT} neurons. For each stimulation trial, EEG was analyzed for 6 min with a 2-minute baseline, and the light-on time was 20 s at 20 Hz. The percentages of NREM sleep, REM sleep, and wakefulness were analyzed during the short-stimulation experiment. (G) Time course of wake, REM and NREM sleep during one-hour optogenetic activation of VP^{ChAT} neurons. The blue column indicates the light stimulation period of the stimulation group. (n = 6 mice, using repeated-measures ANOVA, followed by Tukey *post hoc* test).

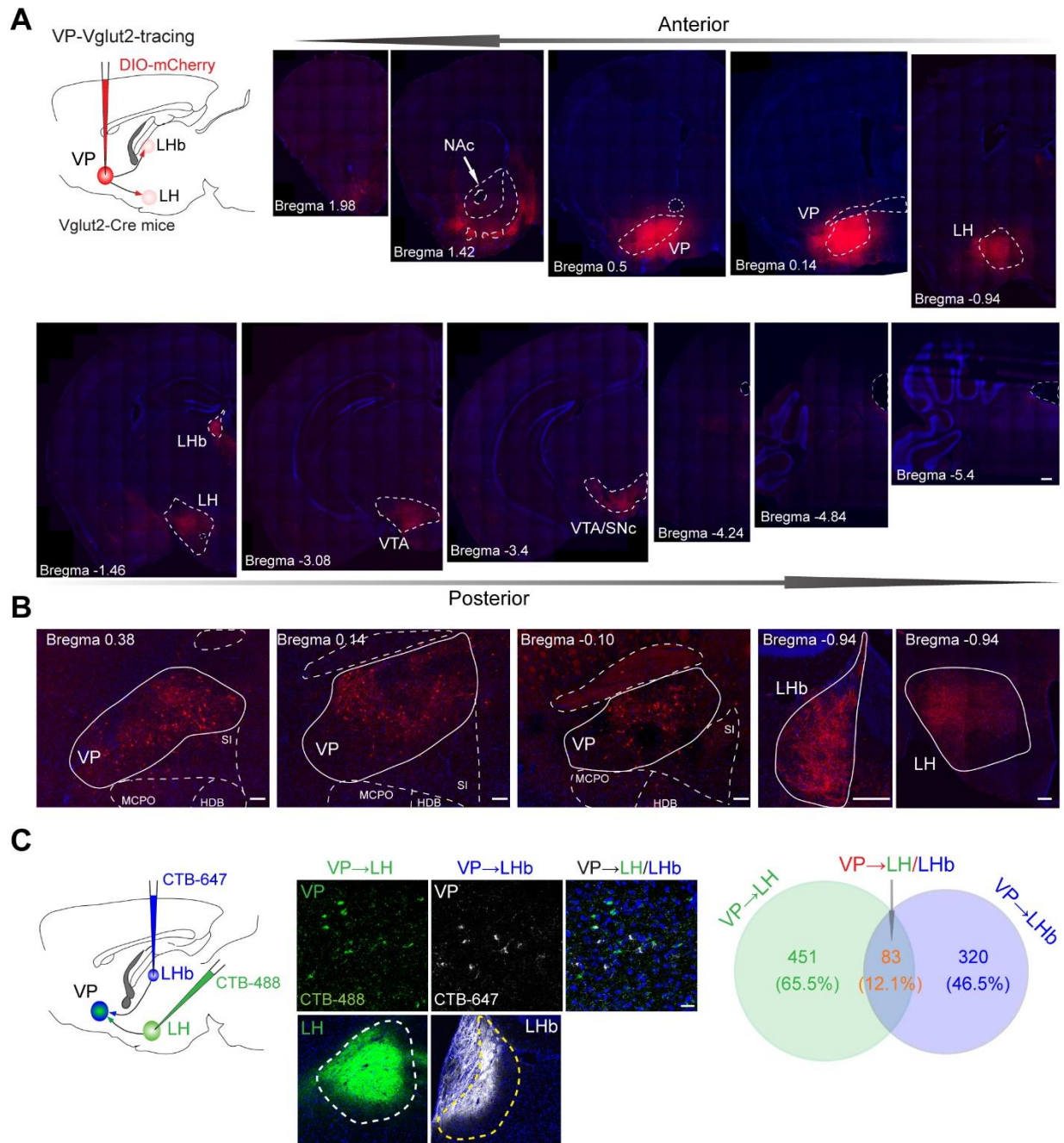


Figure S3 Anterograde and retrograde tracing of VP projection, Related to Figure 5 and Figure 6.

(A) Anterograde tracing of VP^{Vglut2} projections. AAV-hSyn-DIO-mCherry was unilaterally injected into the VP, and whole brain mCherry+ terminals of VP^{Vglut2} neurons were

imaged. Scale bar = 100 μm . (B) Enlarged figures showed mCherry in the injection site of VP and projections in the LHb and LH. Scale bars = 100 μm . (C) Left: Schematic of the experimental protocol. Retrograde tracing of VP-LH and VP-LHb projections. CTB-488 and CTB-647 were unilaterally injected into the LH and LHb, respectively. Middle: CTB-488 (green) and CTB-647 (white) positive cell bodies were found in the VP. Scale bar = 100 μm . Right: Percentages of CTB-488 positive, CTB-647 positive, and double-labeled cells out of the total CTB labeled cells in the VP. $n = 4$ mice.

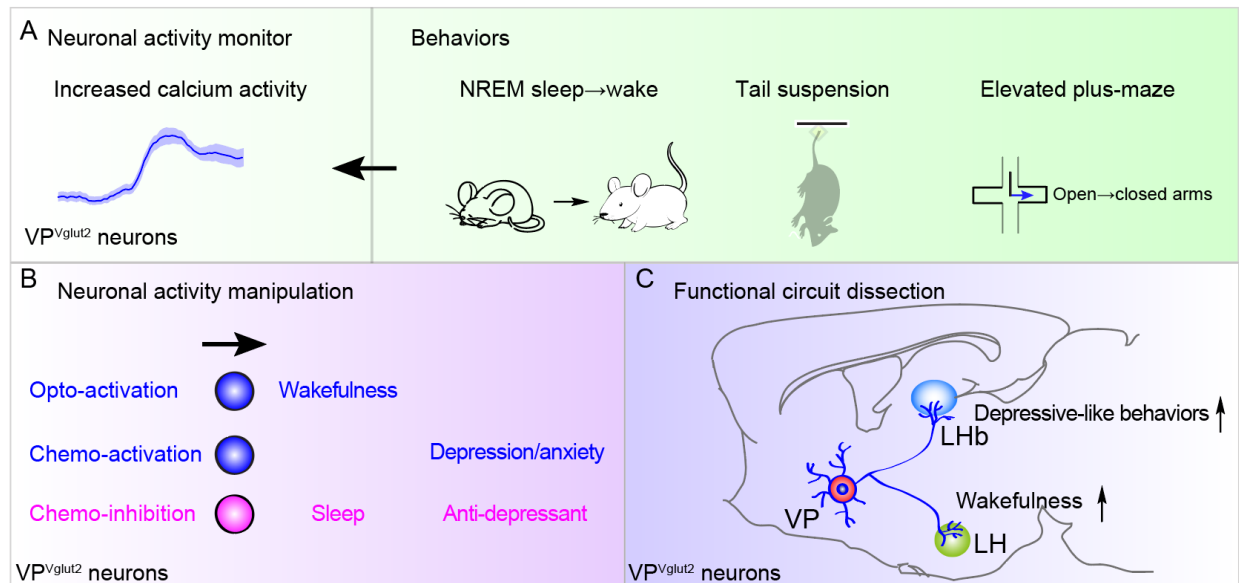


Figure S4. Summary of separated VP^{Vglut2} projections regulate wakefulness and depressive-like behaviors, Related to all Figures.

(A) Increased calcium activity of VP^{Vglut2} neurons in NREM sleep to wake transitions and depressive-like behaviors, suggesting activity of VP^{Vglut2} neurons is linked to wakefulness related to depressive-like behaviors. (B) Activity manipulation of VP^{Vglut2} neurons demonstrates the causal role of VP^{Vglut2} neurons in the regulation of wakefulness and

depressive/anxiety-like behaviors. (C) Functional circuit dissection reveals that VP^{Vglut2} neurons regulate wakefulness and depressive-like behaviors through separated LH and LHb pathways.